

Article

Synthesis of some Cd(II) and Zn(II) complexes of a tetraazamacrocyclic ligand and their antimicrobial activities

Ranjit K. Nath^{1*}, Tapashi G. Roy² and R.K. Sutradhar¹

¹Department of Chemistry, Faculty of Engineering & Technology, Chittagong University of Engineering & Technology (CUET), Chittagong-4349, Bangladesh

²Department of Chemistry, University of Chittagong, Chittagong-4331, Bangladesh

*Corresponding author: Dr. Ranjit K. Nath, Department of Chemistry, Faculty of Engineering & Technology, Chittagong University of Engineering & Technology (CUET), Chittagong-4349, Bangladesh. Phone: +8801817750388; E-mail: rkn_chem@yahoo.com

Received: 31 May 2017/Accepted: 23 August 2017/ Published: 31 August 2017

Abstract: Synthetic macrocycles specially the tetraazamacrocycles and their complexes have attracted considerable interests owing to their wide variety of applications. The ligand, 3, 10-C-meso-3,5,7,7,10,12,14,14-octamethyl-1,4,8,11-tetraazacyclotetradeca-4,11-diene (L^1), upon reaction with CdI_2 , $Zn(ClO_4)_2$, and $Zn(CH_3COO)_2$ produces corresponding square pyramidal cadmium (II) and zinc (II) complexes of formula $[ML^1X]Y_n$, ($M = Cd$ or Zn ; $X = I, CH_3COO$ or H_2O ; $Y = I, ClO_4$ or CH_3COO ; $n = 1$ or 2). Among them, $[CdL^1]I$ and $[ZnL^1(H_2O)](ClO_4)_2$ undergo substitution reactions with $KSCN$ and $NaNO_2$, respectively to produce octahedral trans-diisothiocyanatocadmium(II) complex, trans- $[CdL^1(NCS)_2]$ and square pyramidal mononitratocadmium(II) nitrate complex, $[ZnL^1(NO_2)](NO_2)$. Antifungal and antibacterial activities of these complexes against some of phytopathogenic fungi and bacteria have been investigated in this study.

Keywords: macrocyclic ligand; cadmium (II) & zinc (II) complexes; antimicrobial activities

1. Introduction

Organometallic macrocyclic compounds like tetraazamacrocycles and their complexes have attracted considerable interests due to their wide variety of applications: such as in magnetic resonance imaging (MRI) and radio immunotherapy pharmacological, industrial and analytical fields (Bembi *et al.*, 1991; Roy *et al.*, 2011, 2010, 2010a, 2008). Recent interests have been stimulated by the diagnostic and therapeutic medicinal applications of transition metal complexes of macrocyclic ligands. Moreover concerning biological applications, metal complexes of fourteen membered tetraazamacrocyclic ligands have also been explored for their antifungal and antibacterial (Roy *et al.* 2009; Shin *et al.* 2007) activities as well their use as anticancer and antitumor drugs (Kim *et al.* 2005; Roy *et al.* 2006).

Against this background, a number of copper, nickel and cobalt complexes of 3, 10-C-meso-Me₈-tetraazacyclotetradecadiene (L^1) (Figure 1) have been synthesized and explored for their anti-fungal and antibacterial activities (Horn *et al.* 2001; Roy *et al.* 2011a). Template synthesis of four coordinate copper (II) and nickel (II) complexes has also been achieved (Bembi *et al.* 1988). However cadmium (II) and zinc (II) complexes of this ligand have not been reported so far. Thus the present investigation describes the synthesis, characterization, antifungal and antibacterial activities of some new cadmium (II) and zinc (II) complexes of 3, 10-C-meso-Me₈-tetraazacyclotetradecadiene (L^1).

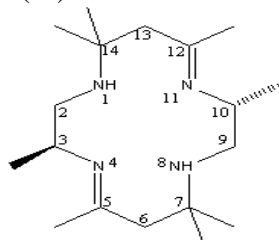


Figure 1. Structure of macrocyclic ligand L^1 .

2. Materials and Methods

All the chemicals and solvents used in the reactions were of AR grade and obtained from commercial sources (Merck, Germany). The solvents were dried using standard literature procedures. Microanalyses of C, H, N and S of complexes have been carried out on a C, H, N, S analyzer at the Inorganic Research Laboratory of the Institut der Anorganische and Angewandte Chemie, Hamburg Universitaet, Germany. The infrared spectra of the metal complexes were taken as KBr discs in the range 4000-400 cm^{-1} at BCSIR laboratory, Dhaka. Electronic spectra of the samples were recorded on a Shimadzu UV-visible spectrophotometer at BCSIR laboratory Chittagong, Bangladesh. Conductance measurements of the metal complexes were done in CHCl_3 , DMF and DMSO solutions using HANNA instrument with HI 8820N conductivity cell at the University of Chittagong. The $^1\text{H-NMR}$ spectra were recorded in CDCl_3 and DMSO with a 400 MHz Bruker DPX-400 spectrometer using TMS as internal standard at the BCSIR Laboratory, Dhaka, Bangladesh. Magnetic measurements were carried out with a Gouy balance, calibrated against $\text{Hg}[\text{Co}(\text{NCS})_4]$; susceptibilities were corrected for diamagnetic increments.

2.1. Synthesis of macrocycles

Synthesis of the parent ligand, 3,10-C-meso- 3,5,7,7,10,12,14,14-octamethyl-1,4,8,11.- tetraazacyclotetradeca-4,11-diene dihydroperchlorate, $\text{L}^1 \cdot 2\text{HClO}_4$ and extraction of free base L^1 were carried out according to the literature (Bembi *et al.* 1989; Roy *et al.* 2010a, 2009, 2008, 2006).

2.2. Synthesis of cadmium(II) complexes

2.2.1. Synthesis of $[\text{CdL}^1\text{I}]\text{I}$

The free ligand L^1 (0.308 g, 1.0 mmol) and cadmium (II) iodide (0.366g, 1.0 mmol) were dissolved separately in hot methanol (40 mL) and mixed. The reaction mixture was heated for 30 min on a steam bath to ensure the completion of the reaction and then allowed to cool. After one day the white product $[\text{CdL}^1\text{I}]\text{I}$ was filtered off, washed with methanol followed by diethyl ether and dried in desiccators over silica gel. Decomposition point: 144°C. Yield 65% (found: C, 32.08; H, 5.39; N, 8.33%; $\text{C}_{18}\text{H}_{36}\text{N}_4\text{CdI}_2$ requires C, 32.04; H, 5.38; N, 8.30%).

2.2.2. Synthesis of axial ligand substitution product, $[\text{CdL}^1(\text{SCN})_2]$ from $[\text{CdL}^1\text{I}]\text{I}$

A suspension of $[\text{CdL}^1\text{I}]\text{I}$ (0.674 g, 1.0 mmol) in hot methanol (40 mL) was added to a solution of KSCN (0.194 g, 2.0 mmol) in hot methanol (40 mL) and the mixture was heated for 30 min on a steam bath and then allowed to cool. After one hour the white product $[\text{CdL}^1(\text{SCN})_2]$ was filtered off, washed with methanol followed by diethyl ether and dried in a desiccator over silica gel. Decomposition point: 164°C. Yield 50% (found: C, 44.93; H, 6.06; N, 15.55%; $\text{C}_{20}\text{H}_{36}\text{N}_6\text{S}_2\text{Cd}$ requires C, 44.73; H, 6.76; N, 15.65%).

2.3. Synthesis of zinc(II) complexes

2.3.1. Synthesis of $[\text{ZnL}^1(\text{H}_2\text{O})](\text{ClO}_4)_2$

A solution of ligand L^1 (0.308 g, 1.0 mmol) in hot methanol (40 mL) was mixed with a solution of zinc (II) perchlorate hexahydrate (0.372g, 1.0 mmol) in hot methanol (40 mL). The resulting solution was refluxed for 30 min on a steam bath and then allowed to cool. After one day the white product $[\text{ZnL}^1(\text{H}_2\text{O})](\text{ClO}_4)_2$ was filtered off, washed with methanol followed by diethyl ether and dried in a desiccator over silica gel. Decomposition point: 164°C. Yield 60% (Found: C, 36.86; H, 6.32; N, 9.39%; $\text{C}_{18}\text{H}_{38}\text{N}_4\text{ZnCl}_2\text{O}_9$ requires C, 36.59; H, 6.48; N, 9.48%).

2.3.2. Synthesis of axial ligand substitution product, $[\text{ZnL}^1(\text{NO}_2)](\text{NO}_2)$ from $[\text{ZnL}^1(\text{H}_2\text{O})](\text{ClO}_4)_2$

A suspension of $[\text{ZnL}^1(\text{H}_2\text{O})](\text{ClO}_4)_2$ (0.590 g, 1.0 mmol) in hot methanol (40 mL) and a solution of NaNO_2 (0.138 g, 2.0 mmol) in hot methanol (40 mL) were mixed. The reaction mixture was refluxed for 30 min on a steam bath and then allowed to cool. After one hour the white product $[\text{ZnL}^1(\text{NO}_2)](\text{NO}_2)$ was filtered off, washed with methanol followed by diethyl ether and dried in desiccators over silica gel. Melting point: above 220°C. Yield 70% (found C, 46.26; H, 7.8.10; N, 17.92%; $\text{C}_{18}\text{H}_{36}\text{N}_6\text{ZnO}_4$ requires C, 46.40; H, 7.79; N, 18.04%).

2.3.3. Synthesis of $[\text{ZaL}^1(\text{CH}_3\text{COO})](\text{ClO}_4)$

To a filtered solution of zinc (II) acetate dihydrate (0.219 g, 1.0 mmol) in hot methanol (40 mL), a suspension of ligand salt $\text{L}^1 \cdot 2\text{HClO}_4$ (0.509 g, 1.0 mmol) in the same solvent (40 mL) was added. A white product separated out after heating for 30 min. The reaction mixture was heated for further 30 minutes on a steam bath while the volume was reduced to 40 cm^3 and then allowed to cool. After one day the white product

$[\text{ZnL}^1(\text{CH}_3\text{COO})](\text{ClO}_4)$ was filtered off, washed with methanol followed by diethyl ether and dried in a desiccator over silica gel. Melting point: above 220°C. Yield 68% (found: C, 45.28; H, 7.41; N, 10.49%) $\text{C}_{20}\text{H}_{39}\text{N}_4\text{ZnClO}_6$, requires C, 45.12; H, 7.38; N, 10.52%).

2.4. Antifungal activities

The test organisms are phytopathogenic. For this reason, all steps of the work were done with high precaution and aseptic condition. PDA was used as a growth medium for the test. DMSO and chloroform was used as a solvent initially to prepare solution of the ligand and complexes. Such solutions were then mixed with the sterilized PDA to maintain desired concentration (0.01%) of the compounds and the mixture (20 cm³) was poured in each Petri dish. Linear growth of the fungus was measured in mm after five days of incubation at (25 ± 2) °C.

2.5. Antibacterial activities

Antibacterial activities of these complexes against selected bacteria were assessed by the disc diffusion method. Paper disc of 6 mm in diameter and Petri plate of 70 mm in diameter were used throughout the experiment. Pour plates were made with sterilized melted NA (45 °C) and after solidification of pour plates, the test organisms (suspension) were spread uniformly over the pour plate with sterilized glass rod separately. The paper discs after soaking with test chemicals (1% in CHCl_3) were placed at the center of the inoculated pour plate. A control plate was also maintained in each case with CHCl_3 . The plates firstly were kept for 4 hours at low temperature (4 °C) and the test chemicals diffused from disc to the surrounding medium by this time. The plates were then incubated at (35±2) °C for growth of test organisms and were observed at 24-hour intervals. The activity is expressed in terms of diameter of zone of inhibition in mm.

3. Results and Discussion

On the basis of MS, ¹H, ¹³C, ¹H- NMR spectra and X-ray crystallography the structure of 3,10-C-ineso-3,5,7,7,10,12,14,14-octamethyl-1,4,8,11- tetraazacyclotetradeca-4,11-diene (L^1) was established as indicated in Figure 1 (Bembi *et al.* 1989; Roy *et al.* 2010a, 2009, 2006). The free ligand L^1 interacts with CdI_2 , and $\text{Zn}(\text{ClO}_4)_2 \cdot 6\text{H}_2\text{O}$ in methanolic solution to produce square pyramidal $[\text{CdL}^1\text{I}]$ and $[\text{ZnL}^1(\text{H}_2\text{O})](\text{ClO}_4)$ respectively, whereas the ligand salt $\text{L}^1 \cdot 2\text{HClO}_4$ reacts with $\text{Zn}(\text{CH}_3\text{COO})_2$ dihydrate to yield square pyramidal $[\text{ZnL}^1(\text{CH}_3\text{COO})](\text{ClO}_4)$. Among these complexes, $[\text{CdL}^1\text{I}]$ and $[\text{ZnL}^1(\text{H}_2\text{O})](\text{ClO}_4)_2$ undergo substitution reactions with KSCN and NaNO_2 , respectively, to produce octahedral trans- diisothiocyanatocadmium(II) complex trans- $[\text{CdL}^1(\text{NCS})_2]$ and square pyramidal mononitratozinc(II) nitrate complex $[\text{ZnL}^1(\text{NO}_2)](\text{NO}_2)$, respectively. However $[\text{CdL}^1\text{I}]$ did not undergo substitution reactions with KNO_3 , KCl and KBr . Similar results were found for $[\text{ZnL}^1(\text{H}_2\text{O})](\text{ClO}_4)_2$. The reasons of inertness of these complexes toward substitution reactions with the mentioned reagents are not clearly understood yet. All these compounds have been characterized by IR, UV-vis and NMR spectroscopy, as well as by analytical, magnetochemical and conductance measurements. All these complexes were found to be diamagnetic as expected for d^{10} system. The electronic spectra of these complexes do not exhibit any d-d band as expected (Hazari *et al.* 2006; Roy *et al.* 2007). The spectra only showed metal-nitrogen (M-N) charge transfer bands. Since infrared spectra of these complexes could not be run at a range lower than 400 cm^{-1} , so some of the IR bands due to metal-ligands (axial) stretch could not be recorded. The IR, ¹H-NMR and molar conductivity data are summarized in Tables 1, 2 and 3, respectively.

3.1. Cadmium (II) complexes

3.1.1. Monoiodocadmium (II) iodide complex

Reaction of methanolic solution of free ligand L^1 with cadmium (II) iodide produced a white complex, which on the basis of analytical data was formulated as $[\text{CdL}^1\text{I}]$. The infrared spectrum of this complex showed (Table 1) ν_{NH} band at around 3217 cm^{-1} and other characteristic bands for $\nu_{\text{C-N}}$, $\nu_{\text{C-C}}$, $\nu_{\text{C-H}}$, ν_{CH_3} , and $\nu_{\text{Cd-N}}$ at 1655 cm^{-1} , 1161 cm^{-1} , 2966 cm^{-1} , 1369 cm^{-1} and 513 cm^{-1} respectively. Since the spectrum was not run below 400 cm^{-1} , so the expected Cd-I band around 260 cm^{-1} could not be recorded.

Table 1. Selected IR bands of the complexes.

Complexes	Assignment(cm^{-1})						Other bands
	$\nu_{\text{N-H}}$	$\nu_{\text{C-H}}$	$\nu_{\text{C=N}}$	ν_{CH_3}	$\nu_{\text{C-C}}$	$\nu_{\text{M-N}}$	
$[\text{CdL}^1\text{I}]$	3217s	2966m	1655vs	1369s	1161m	513w	-----
$[\text{CdL}^1(\text{SCN})_2]$	3217s	2966m	1654vs	1369s	1161s	513w	2015vs, ν_{CN} ; 840m, ν_{CS} ; 480m, ν_{NCS} 3473vs, ν_{OH} ;
$[\text{ZnL}^1(\text{H}_2\text{O})](\text{ClO}_4)_2$	3188s	2981m	1660vs	1394s	1226s	532w	1660vs, ν_{HOH} ; 1116vs, 624vs, ν_{ClO_4} 1458s, $\nu_{\text{asym}(\text{NO}_2)}$;
$[\text{ZnL}^1(\text{NO}_2)](\text{NO})_2$	3122s	2850m	1650vs	1382s	1145s	534w 430w	1332m, $\nu_{\text{sym}(\text{NO}_2)}$; 835w, $\nu_{(\text{NO}_2)}$
$[\text{ZnL}^1(\text{CH}_3\text{COO})](\text{ClO}_4)$	3190s	2915m	1661vs	1394s	1226s	559w	1129vs, 624s, ν_{ClO_4} ; 1602s, $\nu_{\text{CH}_3\text{COO}^-}$

S= strong, m= medium, vs= very strong, w= weak

The $^1\text{H-NMR}$ spectrum of this complex displayed (Table2) four sharp singlets at 1.26 ppm, 1.36 ppm, 1.90 ppm and 2.09 ppm corresponding to 6H, 6H, 6H and 4H, respectively. The singlets at 1.26 ppm and 1.36 ppm were assigned to the gem-dimethyl groups having equatorial and axial orientation. The third singlet at 1.90 ppm was due to 6H equatorially oriented methyl protons on sp^2 carbons at C5 and C12 positions. The fourth singlet at 2.09 ppm corresponding to 4H was attributed to CH, protons at C6 and C13. However appearance of only upfield doublet at 1.05 ppm was attributed to the equatorially oriented chiral methyl protons on C3 and C10 positions. The other multiplets at 2.75 ppm, 3.20 ppm and 3.95 ppm were presumably due to methylene, methine and NH protons.

Table 2. Selected $^1\text{H-NMR}$ data for the complexes.

Complexes	Types of protons			
	Geminal dimethyl $\delta(\text{ppm})$	Methyl protons on sp^2 carbons $\delta(\text{ppm})$	Methyl protons on chiral carbon $\delta(\text{ppm})$	CH_2 , CH and NH $\delta(\text{ppm})$
$[\text{CdL}^1\text{I}]$	1.26 (s, 6H, e), 1.36 (s, 6H, a)	1.90 (s, 6H, e)	1.05 (d, 3H, e)	2.09 (S,4H), 2.75(m), 3.20 (m)
$[\text{CdL}^1(\text{SCN})_2]$	1.27 (s, 6H, e), 1.37 (s, 6H, a)	1.90 (s, 6H, e)	1.05 (d, 6H, e)	2.40 (m), 2.77(m), 3.25 (m), 3.78 (m)
$[\text{ZnL}^1(\text{H}_2\text{O})_2](\text{ClO}_4)_2$	1.26 (s, 6H, e), 1.36 (s, 6H, a)	1.89 (s, 6H,e)	1.05 (d, 6H, e)	2.43 (m), 2.99 (m), 3.25 (m), 3.77 (m)

s = singlet, d = doublet, m = multiplet, a = axial, e = equatorial

The molar conductivity values (Table 3) of $70 \text{ ohm}^{-1}\text{cm}^2\text{mol}^{-1}$ in DMF and $62 \text{ ohm}^{-1}\text{cm}^2\text{mol}^{-1}$ in DMSO solution indicate that the complex is 1:1 electrolyte in nature. This evidence supports a square pyramidal geometry (Figure 2) for this complex.

Table 3. Conductivity data for the complexes.

Complexes	Solubility	Conductance in DMF ($\text{ohm}^{-1}\text{cm}^2\text{mole}^{-1}$)	Conductance in DMSO ($\text{ohm}^{-1}\text{cm}^2\text{mole}^{-1}$)	Conductance in CHCl_3 ($\text{ohm}^{-1}\text{cm}^2\text{mole}^{-1}$)
$[\text{CdL}^1\text{I}]$	DMSO, DMF	70	62	-----
$[\text{CdL}^1(\text{SCN})_2]$	CHCl_3	-----	-----	0
$[\text{ZnL}^1(\text{H}_2\text{O})](\text{ClO}_4)_2$	DMSO, DMF	158	193	-----
$[\text{ZnL}^1(\text{NO}_2)](\text{NO})_2$	DMSO, DMF	105	85	-----
$[\text{ZnL}^1(\text{CH}_3\text{COO})](\text{ClO}_4)$	DMSO, DMF	125	68	-----

'-' means insoluble

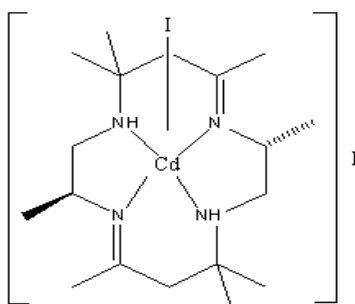


Figure 2. Structure of $[\text{CdL}^1\text{I}]$.

3.1.2. Trans-diisothiocyanato cadmium (II) complex

The above mentioned complex $[\text{CdL}^1\text{I}]$ had undergone substitution and addition reactions simultaneously with KSCN, producing a white product of formula, $[\text{CdL}^1(\text{SCN})_2]$. The infrared spectrum of this complex shows ν_{NH} band at 3217 cm^{-1} , ν_{CN} band at 1654 cm^{-1} and other characteristic bands for $\nu_{\text{C-C}}$, $\nu_{\text{C-H}}$, ν_{CH_3} , and $\nu_{\text{Cd-N}}$ at 1161 cm^{-1} , 2966 cm^{-1} , 1369 cm^{-1} and 513 cm^{-1} , respectively. The spectrum further showed ν_{CN} band at 2015 cm^{-1} , ν_{CS} at 840 cm^{-1} and ν_{NCS} band at 480 cm^{-1} , indicating coordination by the -NCS moiety.

The $^1\text{H-NMR}$ spectrum of this complex showed three sharp singlets at 1.27 ppm, 1.37 ppm and 1.90 ppm each corresponding to 6H. The first two singlets at 1.27 ppm and 1.37 ppm were assigned to the protons of gem-dimethyl groups on C7 and C14 having equatorial and axial orientations and the third downfield singlet at 1.90 ppm was due to the protons of methyl groups on sp^2 carbons. The spectrum also showed singlet at 1.05 ppm corresponding to 6H. The position of this upfield doublet was assigned to the equatorial chiral methyl protons. The other multiplets at 1.85 ppm, 2.40 ppm and 2.77 ppm, 3.01 ppm and 3.78 ppm were attributed to the methylene, methine and NH protons.

This observation indicated that though axial substitution as well as axial addition had taken place on square pyramidal $[\text{CdL}^1\text{I}]$ to form octahedral trans- $[\text{CdL}^1(\text{NCS})_2]$, the stereochemistry of the ligand of the newly formed complex remained the same.

The conductance value of $0\text{ ohm}^{-1}\text{ cm}^2\text{ mol}^{-1}$ for this complex in CHCl_3 strongly supports the nonelectrolytic nature of this complex, indicating coordination by the thiocyanate ions. Thus an octahedral structure (Figure 3) can be assigned for $[\text{CdL}^1(\text{NCS})_2]$.

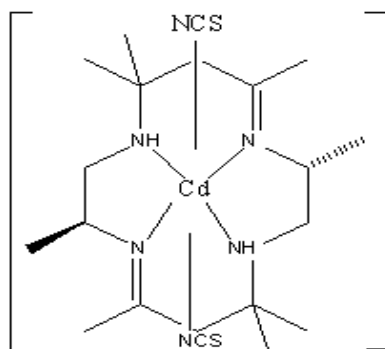


Figure 3. Structure of $[\text{CdL}^1(\text{NCS})_2]$.

3.2. Zinc (II) complexes

3.2.1. Aquazinc (II) diperchlorate complex

Interaction of L^1 with zinc (II) perchlorate hexahydrate in methanolic solution produced white solid product, which on the basis of analytical data coupled with $^1\text{H-NMR}$ results was formulated as $[\text{ZnL}^1(\text{H}_2\text{O})](\text{ClO}_4)_2$. The IR spectrum of $[\text{ZnL}^1(\text{H}_2\text{O})](\text{ClO}_4)_2$ showed ν_{NH} band at 3227 cm^{-1} , $\nu_{\text{C=N}}$ band at 1660 cm^{-1} and other characteristic $\nu_{\text{C-H}}$, $\nu_{\text{C-C}}$ and $\nu_{\text{Zn-N}}$ bands at the expected region (Table 1). The spectrum further showed bands at 1116 cm^{-1} and 624 cm^{-1} which supported the presence of ClO_4^- ion. Presence of ν_{OH} bands at 3473 cm^{-1} and $\nu_{\text{H}_2\text{O}}$ band at 1660 cm^{-1} overlapped with $\nu_{\text{C=N}}$ band were attributed to the presence of coordinated H_2O molecule. The $^1\text{H-NMR}$ spectrum (Table 2) of this complex displayed three sharp singlets at 1.26 ppm, 1.36 ppm and 1.89 ppm each corresponding to 6H. The first two singlets at 1.26 ppm and 1.36 ppm were assigned to the gem-dimethyl protons on C1 and C14 having equatorial and axial orientations and the third downfield singlet at 1.89

ppm was accounted for protons of methyl groups on sp^2 carbons. The spectrum also showed a singlet at 1.05 ppm corresponding to 6H of chiral methyls. The position of this upfield doublet was assigned to the equatorial chiral methyl protons. The other multiplets at 2.43 ppm and 2.99 ppm, 3.23 ppm and 3.77 ppm were due to the methylene, methine and NH protons.

The molar conductivity values (Table 3) of $193 \text{ ohm}^{-1}\text{cm}^2\text{mol}^{-1}$ in DMSO and that of $158 \text{ ohm}^{-1}\text{cm}^2\text{mol}^{-1}$ in DMF solution of this complex were in agreement with a 1:2 electrolytic square pyramidal structure (Figure 4) for $[\text{ZnL}^1(\text{H}_2\text{O})](\text{ClO}_4)_2$.

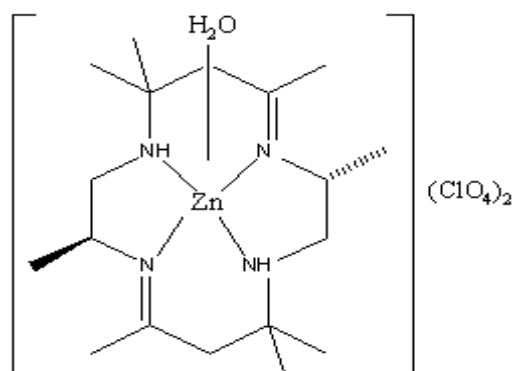


Figure 4. Structure of $[\text{ZnL}^1(\text{H}_2\text{O})](\text{ClO}_4)_2$.

3.2.2. Mononitrozinc(II) nitrite complex

The complex, $[\text{ZnL}^1(\text{H}_2\text{O})](\text{ClO}_4)_2$, had undergone substitution reaction with NaNO_2 in methanolic solution yielding a white product of molecular formula $[\text{ZnL}^1(\text{NO}_2)](\text{NO}_2)$. The infrared spectrum (Table 1) of this complex showed ν_{NH} , $\nu_{\text{C-H}}$, ν_{CH_3} , $\nu_{\text{C-C}}$ and $\nu_{\text{Zn-N}}$ stretching bands in the expected region. Moreover the complex displayed the $\nu_{\text{asym}}(\text{NO}_2)$ and $\nu_{\text{sym}}(\text{NO}_2)$ bands at 1458 cm^{-1} and 1332 cm^{-1} respectively. The spectrum further displayed band at 835 cm^{-1} due to wagging mode of N-bonded nitro complex which was absent in O-bonded nitrito complexes. Presence of $\nu_{\text{Zn-N}}$ band at 430 cm^{-1} and other bands in the proper region strongly supported that the complex was N-bonded nitro complex. Absence of ν_{ClO_4} and ν_{OH} bands and presence of ν_{NO_2} bands demonstrated that ClO_4 and H_2O were completely replaced by NO_2 groups.

The molar conductivity values (Table 3) of $85 \text{ ohm}^{-1}\text{cm}^2\text{mol}^{-1}$ in DMSO solutions and $105 \text{ ohm}^{-1}\text{cm}^2\text{mol}^{-1}$ in DMF of this complex were in agreement with 1:1 electrolytic square pyramidal structure (Figure 5) of the complex.

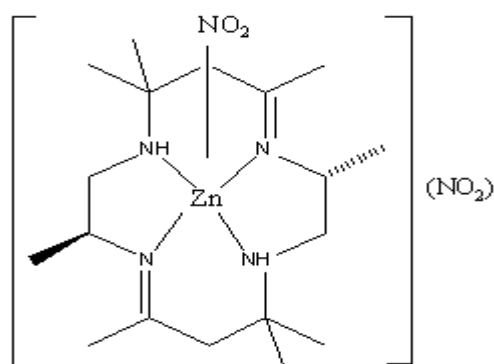


Figure 5. Structure of $[\text{ZnL}^1(\text{NO}_2)](\text{NO}_2)$.

3.2.3. Monoacetatozinc(II) perchlorate complex

Interaction of $\text{L}^1\cdot\text{HClO}_4$ with zinc (II) acetate dihydrate in methanolic solution produced a white solid product. Based on all experimental and analytical data the product was formulated as $[\text{ZnL}^1(\text{CH}_3\text{COO})](\text{ClO}_4)$. The infrared spectrum (Table 1) of this complex showed ν_{NH} band at 3190 cm^{-1} , $\nu_{\text{C=N}}$ band at 1661 cm^{-1} and other characteristic $\nu_{\text{C-H}}$, ν_{CH_3} , $\nu_{\text{C-C}}$ and $\nu_{\text{Zn-N}}$ bands at the expected region. The spectrum further showed bands at 1129 cm^{-1} and 624 cm^{-1} , which supported the presence of ClO_4^- ion. Appearance of a band at around 1602 cm^{-1} indicated the presence of coordinated CH_3COO^- group.

Molar conductivity values (Table 3) of $68 \text{ ohm}^{-1}\text{cm}^2\text{mol}^{-1}$ in DMSO and $125 \text{ ohm}^{-1}\text{cm}^2\text{mol}^{-1}$ in DMF indicated that the complex behaved as 1:1 electrolyte in solution. This behavior supported the square pyramidal structure (Figure 6) of the complex.

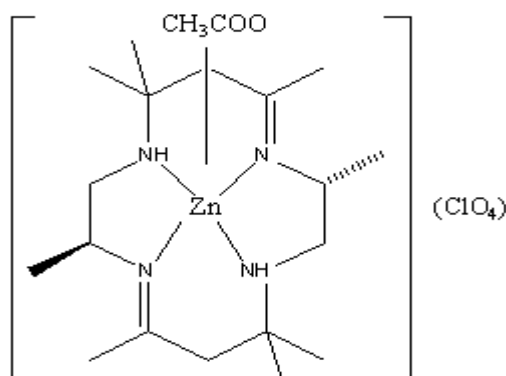


Figure 6. Structure of $[\text{ZnL}^1(\text{CH}_3\text{COO})](\text{ClO}_4)$.

4. Antimicrobial activities

The test organisms are phytopathogenic. For this reason, all steps of the work were done with high precaution and aseptic condition. And the percentage inhibition of mycelia growth of the test fungus/bacteria was calculated by using following equation:

$$\text{Percentage of inhibition} = (\text{CT}/\text{C}) \times 100$$

Here, C = Diameter of the fungal/ bacterial colony in the control

T = Diameter of the fungal/ bacterial colony in the treated

4.1. Fungitoxicity study

Antifungal activities of these complexes are summarized in Table 4. Screenings were conducted against selective phytopathogenic fungi, *Macrophomina phaseolina*, *Alternaria alternate* and *Colletotrichum corcolei*. These fungi are phytopathogens of important crop plants such as jute, chilli, brinjal etc. Control of such pathogens by non-hazardous fungicides has been a major concern, especially as fungi gradually develop resistance to known fungicides. It is evident from the results presented in Table 4 that the macrocycle and its complexes showed some antifungal activity. Generally, previous studies have shown that the activity of the macrocyclic ligands decrease upon coordination (Bembi *et al.* 1991; Roy *et al.* 2010, 2009, 2008; Shin *et al.* 2007) but in the present study, these complexes behaved differently.

Table 4. In-vitro antifungal activities of ligand and metal complexes.

Ligand and complexes	% inhibition of mycelial growth		
	<i>Alacrophomina phaseolina</i>	<i>Alternaria alternate</i>	<i>Colletotrichuns corcolei</i>
L^1	38	10	35
$[\text{CdL}^1]\text{I}$	33	20	50
$[\text{CdL}^1(\text{SCN})_2]$	-	49	35
$[\text{ZnL}^1(\text{H}_2\text{O})](\text{ClO}_4)_2$	18	36	20
$[\text{ZnL}^1(\text{NO}_2)](\text{NO}_2)$	29	23	22
$[\text{ZnL}^1(\text{CH}_3\text{COO})](\text{ClO}_4)$	40	32	36

- means not done

A comparison of the activities of the present ligand and complexes showed that the present compounds showed varied amount of effects on the inhibition of mycelial growth and most of the complexes exhibited greater anti-fungal activities than its corresponding ligand specially against *Alternariaalternate*. It was also observed that different complexes, e.g., acetate, thiocyanate, aqua and nitro complexes of same macrocyclic ligand had different effects on

these organisms. These observations suggested that the nature of metal ion and axial ligand / counter ion played a significant role in the inhibition of micelial growth.

4.2. Antibacterial study

Anti-bacterial activities of the macrocycles and their complexes have so far been studied for few cases only (Bembi *et al.* 1991; Roy *et al.* 2010a; Shin *et al.* 2007; Hazari *et al.* 2006).

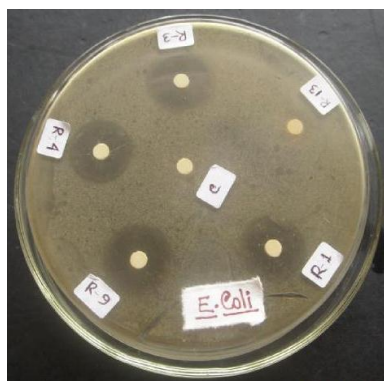


Figure 7. Picture showing inhibition zone against *E. coli* by the synthesized complexes.

Antibacterial activities of these complexes are summarized in Table 5. The results showed that though some of the complexes show different antibacterial activities to a measurable extent but the ligand and some complexes did not show any such activity as compared to our previous study (Roy *et al.* 2009; Shin *et al.* 2007).

Table 5. Antibacterial activities of the ligand and its metal complexes.

Compounds	Diameter of zone of inhibition in mm after 24 hours					
	<i>Bacillus cereus</i>	<i>Bacillus subtilis</i>	<i>Escherichia coli</i>	<i>Shigelladvsent eriae</i>	<i>Bacillus megaterium</i>	<i>Salmonella paratyph</i>
[CdL ^I]I	0	0	8	-	0	0
[CdL ^I (SCN) ₂]	9	8	12	0	9	13
[ZnL ^I (H ₂ O)](ClO ₄) ₂	0	0	13	0	9	0
[ZnL ^I (NO ₂)](NO ₂)	14	11	8	0	0	11
[ZnL ^I (CH ₃ COO)](ClO ₄)	0	0	10	0	0	10

- means not done

5. Conclusions

Inhibition power of the some newly prepared complexes on a particular bacterial growth was measured in these researches. Some of the complexes are found to exhibit higher antibacterial activities than their corresponding ligand. However for a clear understanding of the functions responsible for antibacterial activities of macrocycles, and their complexes, more studies are needed to be performed with a series of analogous ligands and their complexes against a series of bacteria.

Acknowledgement

The authors are thankful to the Ministry of National Science, Information & Communication Technology (NSICT), Bangladesh for the award of research grant to TGR and research fellowship to Ranjit K. Nath.

Conflict of interest

None to declare.

References

- Bembi R, MGB Drew, R Singh and TG Roy, 1991. Polyazamacrocycles. 9. Characterisation of diastereoisomeric trans-[Co(Me₈[14]ane)Cl₂]⁺ complex. *Inorg. Chem.*, 30: 1403-1406.
- Bembi R, TG Roy and AK Jhanji, 1988. Copper(II), nickel(II) and cobalt(III) complexes with new macrocyclic ligands, 6,14-Dimethyl 1,5,9,13-tetraazacyclohexadeca-5, 13-diene(Me₂[16]diene) and C-meso- and C-rac- 6, 14- dimethyl-1,5,9,13- tetraazacyclohexadecane(C-meso- and C-rac-. Me₂[16]ane. *Inorg. Chem.*, 27: 496-500.

- Bembi R, SM Sondhi, AK Singh, AK Jhanji, TG Roy, JW Lown and RGV Ball, 1989. Structure of isomeric 3,5,7,7,10,12,14,14- octamethyl-1,4,8,11 - tetraazacyclotetradecanes. Bull. Chem. Soc. Jpn., 62: 3701-3705.
- Hazari SKS, BK Dey, D Palit, TG Roy and KMD Alam, 2006. Synthesis, characterisation and antimicrobial activities of a NS-chelating ligand with ferrocene backbone and some of its metal complexes. Ceylon J. Sc. (Physical Science), 11: 23-31.
- Horn E, TG Roy, SKS Hazari, BK Dey and ERT Tiekink, 2001. Crystal structure of trans-dinitrito (3, 10 - C - meso - 3, 5, 7, 7, 10, 12, 14, 14 - octamethyl - 1, 4, 8, 11 - tetraazacyclotetradecane) cobalt (III) perchlorate, [Co(Me₈[14]ane)(NO₂)₂]ClO₄. Z. Kristallogr. NCS, 216: 71-72.
- Kim DI, EH Kim, TG Roy, HG Na, ZU Bae and YC Park, 2005. Catalytic activity of asymmetric monobenzoylmonobenzo-tetraazacyclo(14) tetradecinatonicke l(II) complexes: X-ray crystal structure of monobenzo-2,4,9,11-tetramethyl-1,5,8,12- tetraazacyclo[14] tetradecinatonicke (II). J. Coord. Chem., 58: 231-242.
- Roy TG, SKS Hazari, KK Barua, DI Kim, YC Park and ERT Tiekink, 2008. Syntheses, characterization and anti-microbial activities of palladium (II) and palladium (IV) complexes of 3,10-C-*meso*-Me₈[14]diene (L¹) and its reduced isomeric *anes*(L_A, L_B and L_C). Crystal and molecular structure of [PdL¹][Pd(SCN)₄]. Appl. Orgometal. Chem., 22: 637-646.
- Roy TG, SKS Hazari, KK Barua, N Anwar, JS Zukerman and ERT Tiekink, 2010. Syntheses, characterization and anti-microbial studies of cadmium (II) complexes containing 3,10-C-*meso*-Me₈[14]aneC (L_C). Crystal and molecular structure of *cis*- [CdL_C(NO₃)](NO₃). Appl. Org. Chem., 24: 878-887.
- Roy TG, SKS Hazari, KK Barua, SW Ng and ERT Tiekink, 2011. Dichlorido[(4E,11E)-5,7,12,14-tetrabenzyl-7,14-dimethyl-1,4,8,11- tetraaza cyclotetradeca-4,11-diene] cobalt(III) perchlorate. Acta. Cryst., E67: 01722-01723.
- Roy TG, SKS Hazari, KK Barua, P Palit and ERT Tiekink, 2010. 3,10-C-*meso*- 3,5,7,7,10,12,14,14-Octamethyl-4,11-diaza-1,8-diazoniacyclotetradecane bis(perchlorate). Acta. Cryst., E66: 02196-02197.
- Roy TG, SKS Hazari, BK Dey, HA Miah, F Olbrich and D Rehder, 2007. Syntheses and antimicrobial activities of isomers of N(4), N(11)-dimethyl-3,10-C-*meso*- 3,5,7,7,10,12,14,14-octamethyl- 1,4,8,11-tetraazacyclotetradecane and their nickel (II) complexes. Inorg. Chem., 46: 5372-5380.
- Roy TG, SKS Hazari, BK Dey, BC Nath, AF Dutta and D Rehder, 2011. Syntheses, electrolytic behaviour and antifungal activities of Zn(II) complexes of isomers of 3,10-C-*meso*-3,5,7,7,10,12,14,14-octamethyl-1,4,8,11-tetraazacyclotetradecane (L). Crystal and molecular structure of [ZnL_B(NO₃)]NO₃ (L_B = *a,e,a,e*-L). Inorg. Chim.Acta., 371: 63-70.
- Roy TG, SKS Hazari, BK Dey, D Palit and S Chakraborty, 2006. Studies on some transition metal complexes of 3,10-C-*meso*- 3,5,7,7,10,12,14,14-octamethyl- 1,4,8,11- tetraazacyclotetradeca - 4,11-diene. Ceylon J. Sc. (Physical Science), 11: 37-49.
- Roy TG, SKS Hazari, RK Nath, BC Nath and A Manchur, 2009. Synthesis and antimicrobial activities of some cadmium(II) and zinc(II) complexes of 3, 10- C- *meso*- 3, 5, 7, 7, 10, 12, 14, 14- octamethyl - 1, 4, 8, 11 - tetraazacyclotetradecadiene (L¹). J. Bang. Chem. Soc., 22: 111-122.
- Shin SH, DI Kim, YK Lee, YH Lee, ZU Bae, HG Na, TG Roy and YC Park, 2007. Synthesis of asymmetric dibenzoylatedtetraazacyclo[14]annulene-palladium (II) complexes: structure of 3,10-di(*p*-methylbenzoyl)-2,4,9,11- tetramethyl- 1,5,8,12- monobenzotetraazacyclo[14] annulene-palladium(II). Bull. Korean Chem. Soc., 28: 1847-1850.